Composites Science and Technology 151 (2017) 211–218

Contents lists available at ScienceDirect

Composites Science and Technology

journal homepage: http://www.elsevier.com/locate/compscitech

Low thermal and high electrical conductivity in hollow glass microspheres covered with carbon nanofiber–polymer composites

Luis C. Herrera-Ramírez [a], Manuela Cano [a], Roberto Guzman de Villoria [a, b, *]

[a] IMDEA Materials Institute, C/ Eric Kandel 2, 28906 Getafe, Madrid, Spain
[b] FIDAMC, Foundation for Research, Development and Application of Composite Materials, Avda. Rita Levi-Montalcini 29, 28906 Getafe, Madrid, Spain

ARTICLE INFO

Article history:
Received 24 January 2017
Received in revised form
12 June 2017
Accepted 17 August 2017
Available online 23 August 2017

Keywords:
Carbon nanofibers
Hollow glass microspheres
Polymer-matrix composites (PMCs)
Thermal properties
Chemical vapour deposition (CVD)

ABSTRACT

To take advantage of both the low density and thermal conductivity of hollow glass microspheres, and the high mechanical and electrical conductivity of carbon-based nanofillers, micro- and nanosized fillers can be combined into a single composite material. Here we prepared composite materials from hollow glass microspheres (HGMs) and from the same microspheres surrounded by carbon nanofibers (CNFs). By adding 10% wt. of HGM-CNFs to a high-temperature resin we can obtain a low density (0.8 g/cm^3), low thermally (0.17 W/mK) and high electrically conductive ($7\pm3 \times 10^{-4}$ S/m) composite. This novel method demonstrates the possibility to achieve an unusual combination of properties such as low thermal and high electrical conductivity which, along with their light weight and thermal stability, makes these materials promising for aerospace applications or thermoelectric devices.

1. Introduction

There is a need for high-performance polymers with high electrical and low thermal conductivity for aerospace, marine and energy applications. However, this combination of properties is really hard to obtain in a single material.

By adding conducting fillers [1–4] to a polymer matrix, the thermal and electrical conductivity of the resulting composite can be increased. Once these fillers form a conductive network within the polymeric matrix, the electrons can flow through the composite, increasing the thermal and electrical conductivity of the composite. In general, when electrically insulating fillers are added to a polymer [5–8] the thermal conductivity of the composite is modified but not the electrical conductivity.

Opposed effects on the thermal and electrical conductivity can also be obtained by combining insulating and conducting fillers. By adding carbon-based nanomaterials and electrically insulating fillers to a polymer matrix; composites with improved thermal conductivity and high electrical resistivity are obtained [9–11]. This approach, based on the combination of fillers has been followed in the present work using hollow glass microspheres (HGMs) and carbon nanofibers.

Composites containing hollow glass microspheres are very attractive due to their light weight, high thermal stability, and low thermal conductivity [12–15]. Depending on the density (wall thickness) of the HGMs, stiffer composites can be obtained. However, as the interaction between the matrix and HGMs is generally poor, the resultant composites suffer reduced strength, compared with the raw matrix [16,17]. On the other hand, the addition of HGMs to a polymer, e.g., epoxy resin, results in a material with the same electrically insulating behaviour as the matrix but with reduced thermal conductivity [8,12].

Carbon-based nanostructures, such as graphene, graphite nanoplates, graphite oxide, carbon nanofibers (CNFs) and nanotubes are being extensively studied due to their outstanding mechanical, thermal and electrical properties, which make these nanosized structures ideal as nanofillers for aerospace or high-performance composites. To take advantage of both the low density and thermal conductivity of HGMs and the high mechanical and electrical conductivity of carbon-based nanofillers, both micro- and nano-sized fillers can be combined in a single composite material; for example, when 0.3 vol.% of CNFs is added to an epoxy composite with 50 vol.% of HGMs (0.46 g/cm^3), the tensile modulus and strength are increased by 10 and 29%, respectively, compared to the unmodified HGM composite [18]. For an epoxy composite with

* Corresponding author. FIDAMC, Foundation for Research, Development and Application of Composite Materials, Avda. Rita Levi-Montalcini 29, 28906 Getafe, Madrid, Spain.
E-mail address: roberto.guzman@fidamc.es (R. Guzman de Villoria).

http://dx.doi.org/10.1016/j.compscitech.2017.08.020
0266-3538/

10 wt.% of CNFs and 15 vol.% of HGMs (0.22 g/cm^3) the electrical resistance is reduced by 85% while the dielectric constant is increased by four orders of magnitude, compared to the neat resin [19]. The effect of CNFs on the viscoelastic properties [20], as well as on the degradation due to moisture exposure [21] or thermal expansion [22], were also studied.

Several groups have directly grown CNTs on micron-diameter fibres [23–25] and solid particles of different sizes and materials, such as alumina/iron oxide nanoparticles [26], ceramic spheres [27], alumina microparticles [28,29] or silica microparticles [30,31]. However, to our knowledge, there is scarce literature on the growth of carbon nanotubes or nanofibers on micron-scaled hollow glass spheres [32] and only the mechanical (compression) and thermo-mechanical (dynamic mechanical analysis) properties of the produced composites were characterized.

Here we present a method to develop a hybrid composite material with an unusual combination of properties such as improved electrical conductivity and low thermal conductivity. We tailored the composite properties by using a hybrid filler based on carbon nanofibers that were directly synthesized by chemical vapour deposition on micron-sized hollow glass spheres. We also compared our experimental results with analytical models and found a good correlation between the results obtained from both approaches.

2. Methods

2.1. Synthesis of hybrid HGM-CNF particles

Carbon nanofibers were synthesized on the surface of hollow glass microspheres (K20 Glass bubbles, 3M) by means of a chemical vapour deposition process. The catalyst precursor for the growth of carbon nanofibers was iron nitrate nonahydrate ($Fe(NO_3)_3 \cdot 9H_2O$) (Sigma-Aldrich, >98% purity). To coat the surface with the catalyst precursor [24], the microspheres were added to a solution of 50 mM iron nitrate in isopropanol and mechanically mixed for 2 h. Then, the mixture was filtered for overnight and dried at 150 °C for 3 h. After this process, the catalyst precursor-coated HGMs were stored until they were used as substrate for the growth of CNFs.

The treated microspheres were placed in an alumina boat, which was positioned in the middle of a quartz tube and heated by a mobile horizontal tube furnace that allows fast heating and cooling rates. A detailed explanation of the CVD system can be found elsewhere [33]. For the conditioning of the catalyst, the furnace was heated to 600 °C and a flow of 100 sccm of H_2 and 400 sccm of Ar was passed through the quartz tube for 20 min. Afterwards, for the carbon nanofibers growth, the temperature was maintained at 600 °C and a flow of 100 sccm of H_2, 400 sccm of Ar and 200 sccm of C_2H_4 was maintained for 20 min. After this process, the furnace was cooled down under a flow of 1000 sccm of Ar.

2.2. Composite preparation

The resin used as matrix for the preparation of composites was a high-temperature urethane acrylate resin (Crestapol 1234, Scott Bader Company Ltd.). Methyl-ethyl-ketone peroxide solution in diisobuthyl phthalate (Butanox LPT) was used as catalyst (2% by weight of resin) and a solution of cobalt octoate in styrene (Accelerator G) was used as accelerator (2% by weight of resin).

Composites containing 0, 2, 5 and 10 wt.% of HGM and the hybrid material, obtained by the CVD process (HGMs-CNFs), were produced. Resin, catalyst and accelerator were hand-mixed and degassed for 1 min. Then, the appropriate amount of filler was added to the resin and stirred by hand. Finally, the resulting mixture was cast in a silicone mould and cured at room temperature for 48 h, followed by a post-curing cycle of 5 h at 80 °C and 3 h at 195 °C.

2.3. Characterization

2.3.1. Morphology and Raman spectroscopy

The morphologies of the as-received HGMs and the synthesized HGM-CNF particles were analysed by scanning (SEM equipped with an energy-dispersive spectrometer, EVO MA15, Zeiss) and transmission electron microscopy (TEM, JEOL JEM 3000F). The elemental composition of the as-received HGMs was analysed by energy-dispersive spectroscopy (EDS). For SEM and EDS, the particles were lightly pressed onto an adhesive carbon tape and for TEM, a small amount of the hybrid material was dispersed in isopropanol by means of an ultrasonic probe. A drop of the resulting solution was carefully deposited on a TEM carbon-coated Cu grid (LC300-Cu, EMS).

The morphology of the resulting composites was assessed by analysing the fracture surfaces of the manually fractured specimens by light microscopy and scanning electron microscopy (Helios NanoLab 600i, FEI). For SEM, the surfaces of the samples were sputter-coated with a thin layer of gold to avoid electrostatic charge of the sample during the analysis.

The as-received HGMs and the synthesized hybrid fillers were placed on top of thin aluminium foils and analysed by Raman spectroscopy (Micro-Raman spectrometer Renishaw PLC), using a DPSS Nd:YAG green laser (532 nm wavelength). Three measurements were performed per sample. Spectra were obtained for an exposure of 15 s, 5 accumulations, in the range of 200–3500 cm^{-1}, applying a laser power of 5%.

2.3.2. Thermogravimetric analysis and density measurement

The thermal stability of HGMs and the carbon content of the HGMs-CNFs, as well as the thermal stability of the resulting composites, were analysed by using a thermogravimetric analysis (Q50 TA Instruments), during which the samples were heated under air, at a heating rate of 10 °C/min, from room temperature to 800 °C. The residue obtained after the thermogravimetric analysis was used to calculate the actual amount of HGMs and HGMs-CNFs added to the composites. The procedure followed is explained in the Supplementary Information.

The density of the resulting composites was measured by following the ASTM D792-13 standard [34], through the application of the Archimedes' principle. At least three cylindrical samples for each filler content, were first weighted in air and then in distilled water at 24 °C. The theoretical density of composites was also obtained, by applying the rule of mixtures, to compare the experimentally measured densities of the composites with their theoretical densities. The HGM and HGM-CNF weight fractions used to calculate the theoretical densities were those obtained by TGA, as mentioned above. The equations used for the calculation of the filler volume fraction and the theoretical density are available in the Supplementary Information.

2.3.3. Thermal conductivity analysis

The thermal conductivity, thermal diffusivity, and the volumetric heat capacity of the resulting composites were measured at room temperature by applying a transient plane source technique (TPS 2500 S, Hot Disk AB). A thin heater/sensor, with a radius of 2.001 mm, was placed between two identical samples (30 mm diameter and 3 mm thick). The heater/sensor element was first

used as a heat source to increase the temperature of the surrounding sample by applying an output power of 0.01 W. Afterwards, the temperature increase was monitored over a period of time of 20 s by measuring the resistance of the heater/sensor. A detailed description of the transient plane source technique, as well as its theoretical background, can be found in Refs. [35–37]. For each filler content and neat resin at least three measurements were performed. To minimize the effect of the interfacial thermal resistance, the surfaces of the cylindrical samples were polished.

To further analyse the thermal conductivity of the composites, Maxwell's model was applied to predict the theoretical thermal conductivities of HGM and HGM-CNF composites.

2.3.4. Electrical conductivity analysis

To perform the DC electrical conductivity measurements, the disc-shaped specimens used for the thermal conductivity measurements were cut into 3 × 3 × 3 mm^3 parallelepiped samples. The electrical resistance was measured in the in-plane and the through-thickness direction of the samples (Supplementary Information). The corresponding two opposite faces were subjected to a polishing process to ensure a smooth surface. The polished surfaces were coated with silver paint as non-guarded electrodes. The voltage (V) applied to the electrodes was increased between 15 and 40 V, and the I–V slope (Keithley SMU 2450 Graphical series SourceMeter) was fitted with the least-squares method. Electrical conductivity was calculated by normalizing measured slope with sample geometry. An estimation of the percolation threshold for the HGM-CNF composites was obtained. The procedure and equations applied are available in the Supplementary Information. Three samples were measured per volume fraction of filler.

3. Results and discussion

3.1. Characterization of the fillers

3.1.1. Hollow glass microspheres

The EDS analysis of the as-received HGMs, presented in Fig. 1a, revealed that the chemical composition of the particles resemble that of soda-lime-borosilicate glass. The SEM images showed that the as-received HGMs have a size distribution of between approximately 20 and 100 μm. The microspheres were homogeneously dispersed on the carbon adhesive tape and no agglomerates were observed. Only a few of the as-received HGMs were broken (inset in Fig. 1a). The HGMs are thermally stable up to 800 °C, which is well above the CVD synthesis temperature (600 °C), as measured by TGA (Fig. 2a).

3.1.2. Hollow glass microspheres–carbon nanofibers

After the synthesis process, the glass microspheres maintained their spherical shape, as the softening temperature of the particles, i.e., the temperature at which the viscosity of the material reaches a value high enough to allow the deformation of the particle under its own weight [38], was not reached during the CVD process. A certain amount of carbon-based nanostructures, grown by the CVD process, seems to be covering the surface of HGMs (Fig. 1b), although not completely. By SEM and TEM observation, it was found that the synthesized nanostructures were highly heterogeneous. Although most of the synthesized structures (Fig. 1c) were identified as carbon nanofibers (Fig. 1d), a small amount of different carbon-based architectures was also observed in the hybrid material obtained after CVD: hollow carbon nanofibers, nanotubes, and graphitic particles (see Supplementary Information).

From the TGA measurements of the HGM-CNF samples (Fig. 2a) we obtained the carbon content of hybrid fillers and the thermal

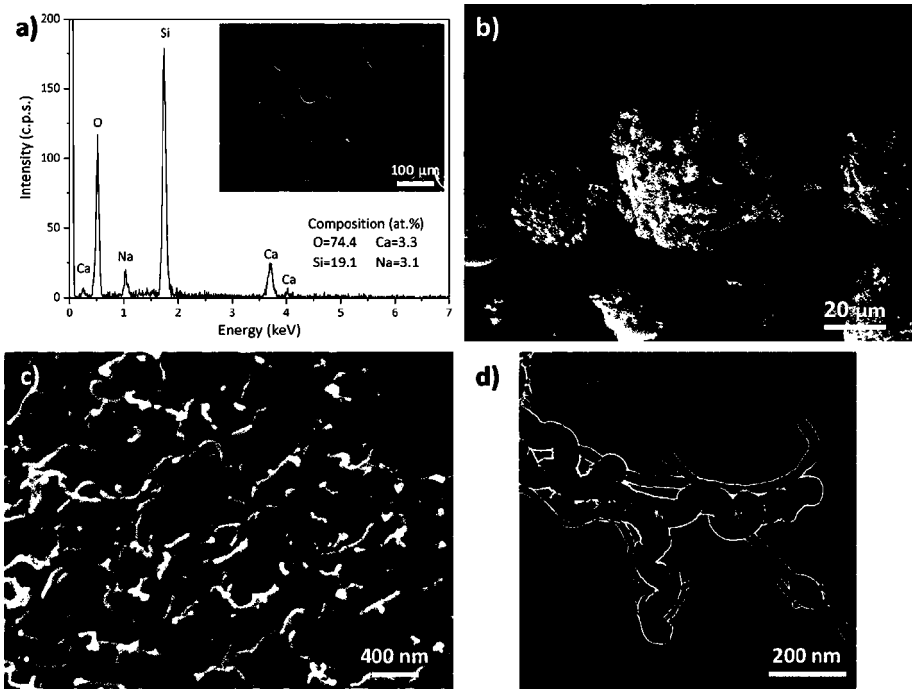

Fig. 1. a) EDS of the as-received HGMs, performed to analyse the chemical composition (in at.%) of the as-received microspheres. The inset shows a SEM image of the as-received HGMs. b) SEM images of the HGMs after the CVD process; the carbon-based nanostructures cover the surface of the HGMs, although not completely. c) High-magnification SEM images of the synthesized carbon nanofibers. d) TEM images of CNFs in the resulting hybrid material.

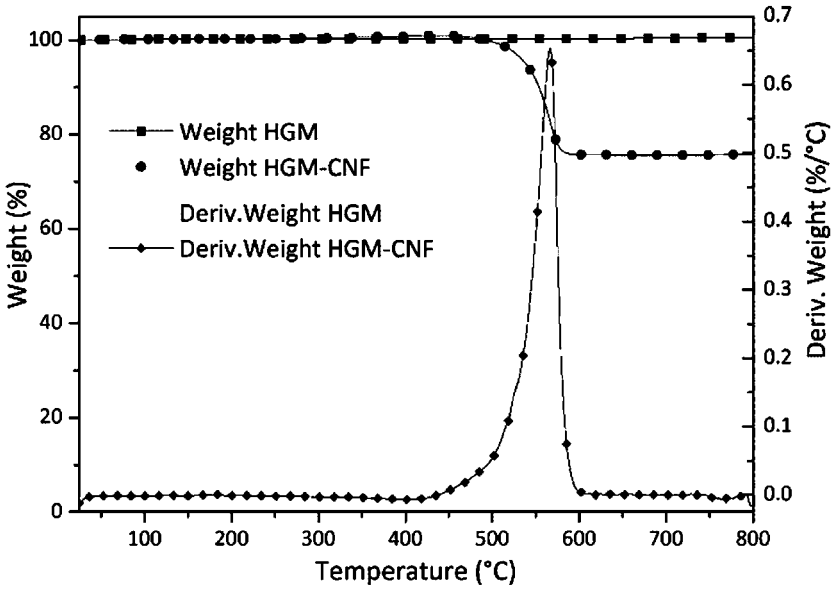

Fig. 2. Weight change and derivative of weight change, as a function of the temperature, of the HGMs and the HGMs-CNFs. The thermal stability up to 800 °C is confirmed for the HGMs. The amount of CNFs, obtained by CVD, is 25 wt.% of the hybrid HGM-CNF material.

stability of the carbon nanostructures. The temperature at which the CNFs started to decompose (onset temperature), was *ca.* 535 °C, similar to onset temperatures for MWNTs (400–600 °C) [39,40]. It was obtained that CNFs constituted 25 wt.% of the total amount of the HGM-CNF material.

3.2. Characterization of composites

3.2.1. Morphology, thermal stability and density

The morphology of the composites was characterized by optical and electronic microscopy of the fractured surfaces. The filler was homogeneously dispersed within the matrix of both HGM and HGM-CNF composites (Fig. 3a–b and Supplementary Information), which was not expected as both fillers were dispersed by hand-stirring. A few microspheres appeared to be damaged, probably due to sample preparation and the manufacturing process. In the HGM-CNFs composites, most of the synthesized CNFs remained located around the HGMs (Fig. 3c–d), and thus was part of the interphase between the matrix and HGMs.

The thermal stability of composites was analysed by thermogravimetric analysis carried out in air. The TGA curves of the samples, presented in Fig. 4, were used to analyse the thermal stability of the

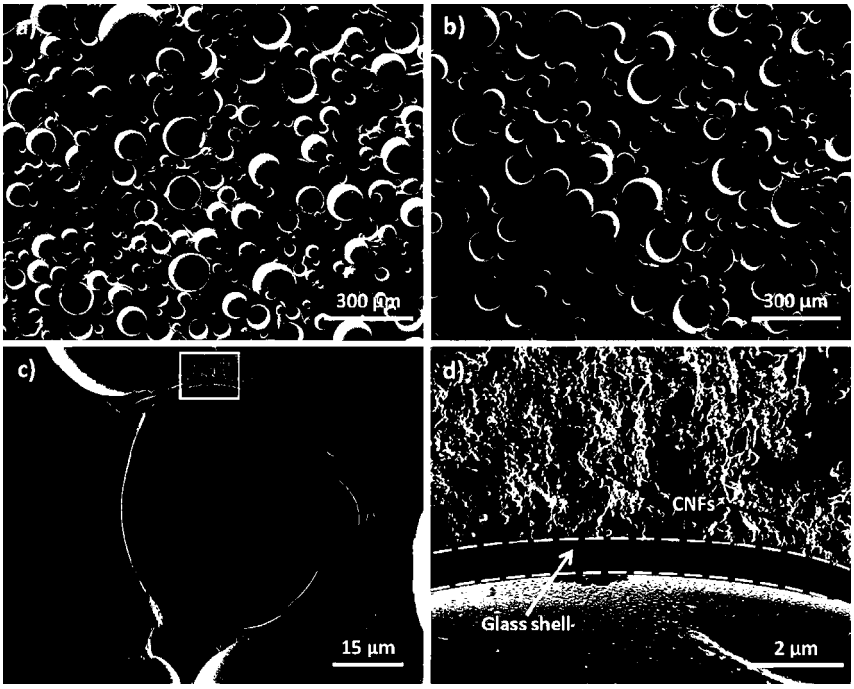

Fig. 3. SEM images of the fractured surfaces of the a) 10 wt.% HGM and b) 10 wt.% HGM-CNF composites; there is a homogeneous dispersion of the HGMs. c) A broken HGM shown in the 10 wt.% HGM-CNF composite and d) the magnified view showing the glass shell and the synthesized CNFs on the HGM surface, which make up part of the HGM-matrix interface. Some CNF agglomerates are dispersed within the matrix and located near the HGM-CNFs.

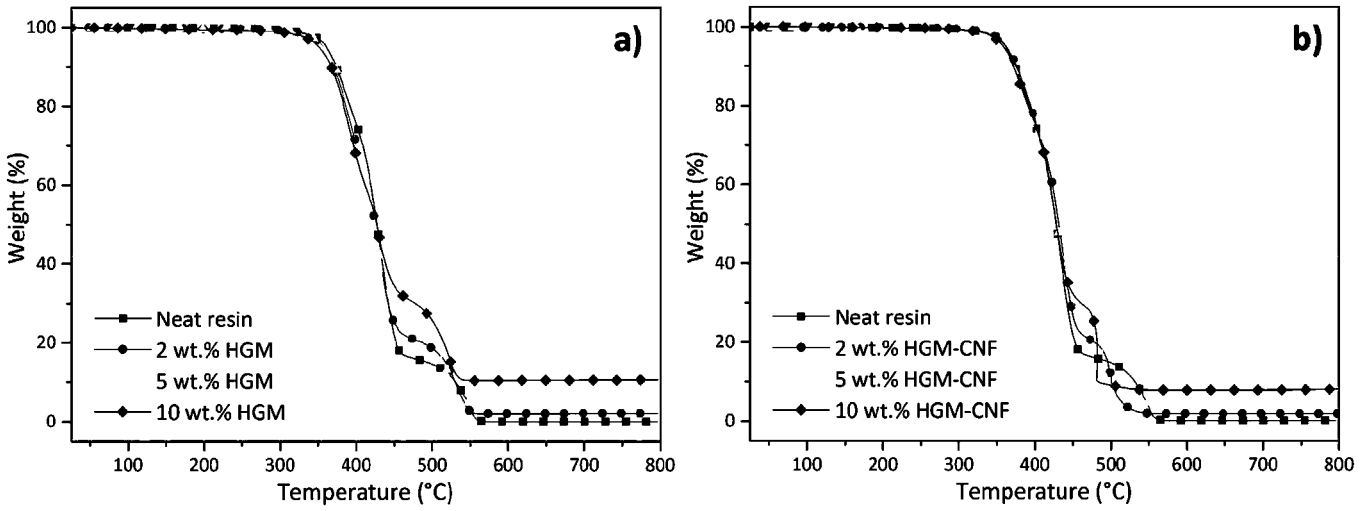

Fig. 4. Weight change, as a function of the temperature, of the a) HGM and b) HGM-CNF composites. The residue left at 650 °C (Table 1), after the degradation process of polymer and CNFs has finished, was used to confirm the amount of HGMs that were added to the composites.

resulting composites and to confirm the amount of filler added to the matrix. As observed, the onset temperature of thermal degradation of the resin (357 °C) is not significantly affected by the addition of HGMs (360–361 °C for all the composites). In the case of the HGM-CNF composites, the onset temperature of thermal degradation was only slightly reduced by the addition of further CNFs; it was 361, 358 and 355 °C for the 2, 5 and 10 wt.% HGM-CNF composites, respectively.

The results obtained from the TGA allowed us to confirm the filler content by measuring the residue left at 650 °C, after the degradation process of polymer and CNFs have finished (Table 1). The addition of HGMs and HGMs-CNFs to the polymeric matrix led to a decrease in the density of the material. As expected, the lowest densities were obtained for the composites with the largest amounts of filler, which were 35% (10% wt. HGM) and 29% (10 wt.% HGM-CNF) lower than the density of the neat matrix. The differences between the theoretical (Table 1) and the experimental amount of filler could be attributed to errors during weighing the filler to be mixed with the resin, porosity of the matrix, or localized heterogeneous dispersion of the filler within the matrix [41,42].

3.3. Thermal behaviour

The effect of the HGMs and the HGMs-CNFs on the thermal behaviour of the neat resin was analysed by the hot-disk technique. The values obtained for the thermal conductivity, k, and thermal diffusivity, λ, are shown in Fig. 5 and Fig. 6. The thermal conductivity of composites decreases with an increased amount of HGMs and HGMs-CNFs added. The neat resin had a thermal conductivity, k_m, of 0.228 W/mK.

For composite materials formed by two phases, i.e. resin and HGMs, Maxwell model was applied to analyse the effective thermal conductivity of the HGM composites. Maxwell model assumes randomly dispersed and non-interacting spheres [43], thus it is only valid for low volume fractions of filler (<10 vol.%) [44]. As observed in Fig. 5a, the results obtained by the application of Maxwell's equation are well in agreement with those experimentally obtained.

For the HGM-CNF composites, the thermal conductivity of the resulting material decreased with the addition of filler. Nevertheless, the thermal conductivity of HGM-CNFs composites is higher than that of the HGM composites for the same amount of filler. This higher thermal conductivity of HGM-CNF composites than HGM composites should be due to the high thermal conductivity of the CNFs [45] and the lower content of HGM per volume fraction of HGM–CNF (Fig. 5), compared with the HGM composite with the same wt.% of filler. For the 10 wt.% HGM composite (*ca.* 40 vol.% HGM) we obtained a thermal conductivity that was 31% lower than for the neat resin, which is in agreement with the values reported for HGM–epoxy [14]. In the case of the composite with 10 wt.% of HGMs-CNFs (*ca.* 34 vol.% HGM) the measured thermal conductivity (0.172 W/mK) is 25% lower than that of neat resin. The same reduction has also been reported for 30 vol.% of HGMs in epoxy composites [14]. It is clear that, regardless of the presence of CNFs within the matrix, the main contribution to the thermal conductivity of the composite is the presence of HGMs.

We also applied the Maxwell model to estimate the thermal conductivity of the resulting HGM-CNF composites. This estimation was done by adjusting the theoretical values obtained from the Maxwell equation (Supplementary Information) to the

Table 1
Analysis of the filler amount and density of the resulting composites. Residue, at 650 °C, obtained after the thermogravimetric analysis of neat resin, HGM, and HGM-CNF composites. The experimental densities were measured according to the ASTM D792-13 standard [34].

Filler amount (wt.%)		Residue (wt.%)	Experimental wt.% HGM/wt.% CNF	Experimental density (g/cm^3)
0		0.2	–/–	1.159
HGMs	2	2.2	2.1/-	1.056
	5	4.9	4.8/-	0.921
	10	10.4	10.3/-	0.752
HGMs-CNFs	2	1.9	1.7/0.6	1.101
	5	3.9	3.7/1.2	1.004
	10	7.9	7.7/2.6	0.823

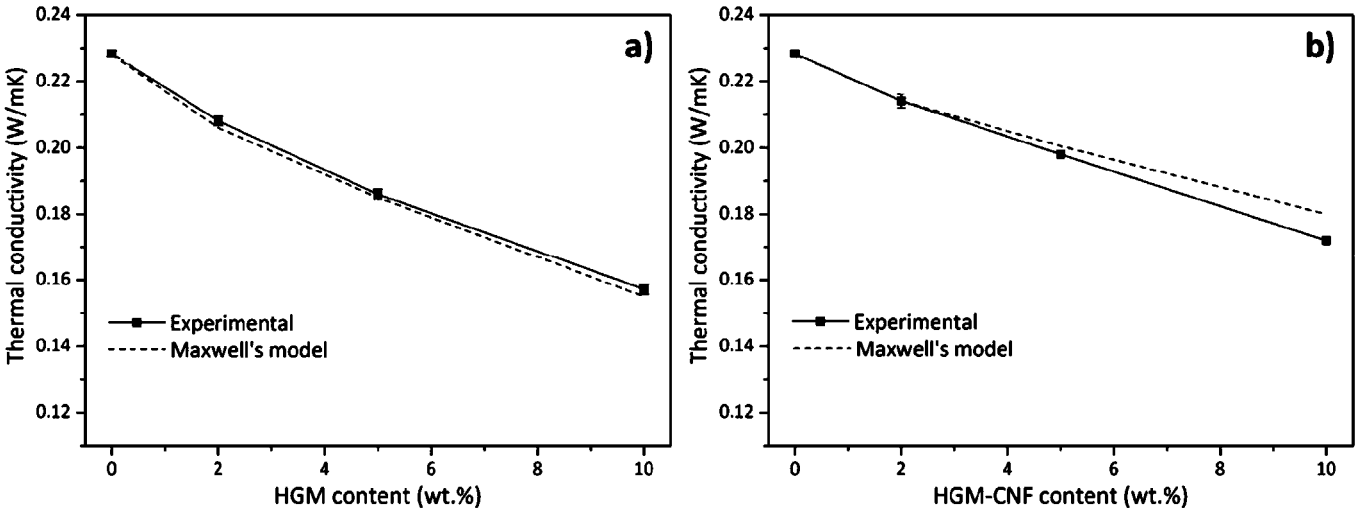

Fig. 5. Analysis of the thermal conductivity of the a) HGM and b) HGM-CNF composites. The experimental results were obtained from the measurements of a hot disk process. The values obtained by the application of the Maxwell's model are also shown for comparison with the experimental values.

experimental thermal conductivity values of the HGM-CNF composites. As mentioned, the Maxwell model is only valid for low volume fractions of filler, thus the value of $k_{HGM-CNF}$ used for the application of the series and parallel models corresponded to the composite with 2 wt,% of HGM, i.e., $k_{HGM-CNF}$ = 0.104 W/mK (Supplementary Information). The obtained results are in agreement with the experimental values, as observed in Fig. 5b.

Along with the addition of HGMs, there are several mechanisms that account for the reduction of the thermal conductivity of HGM-CNF composites. The structure and quality of the CNFs affect the resulting thermal conductivity as defects and presence of amorphous carbon can strongly affect heat conduction [46]. Thermal conductivity is reduced due to the presence of contacts between CNFs and between HGMs and the effect of the interfacial thermal resistance or Kapitza resistance between the CNFs and the matrix, the CNFs and the HGMs, and HGMs and the matrix, which were not taken into account in the applied models [47–50].

The thermal diffusivity, λ, of an homogeneous and isotropic material is given by the ratio between its thermal conductivity and the product of its density and specific heat capacity, c, Eq. (1).

$$\lambda = \frac{k}{\rho c} \tag{1}$$

Thus, the thermal diffusivity, λ, can be understood as the ratio between the ability of heat to flow through the material and its ability to store thermal energy [51].

In the case of HGM composites, it can be observed that the 2 wt.% composite have a λ = 0.166 mm^2/s, which does not significantly differs from that of neat resin (0.167 mm^2/s). However, for the 5 and 10 wt.% composite, λ increases reaching a maximum value of 0.184 mm^2/s for the 10 wt.%.

A HGM consists in a spherical glass shell filled by a gas. The thermal diffusivity of glass is approximately 0.56 mm^2/s, while light gases such as air or He typically have higher thermal diffusivity (22 and 137 mm^2/s, respectively) [51]. Thus, it is reasonable to assume that the thermal diffusivity of HGMs is higher than that of neat resin. This explains the increase in thermal diffusivity of the resulting composites when the HGMs are dispersed within the polymeric matrix. On the other hand, in the case of the HGM-CNF

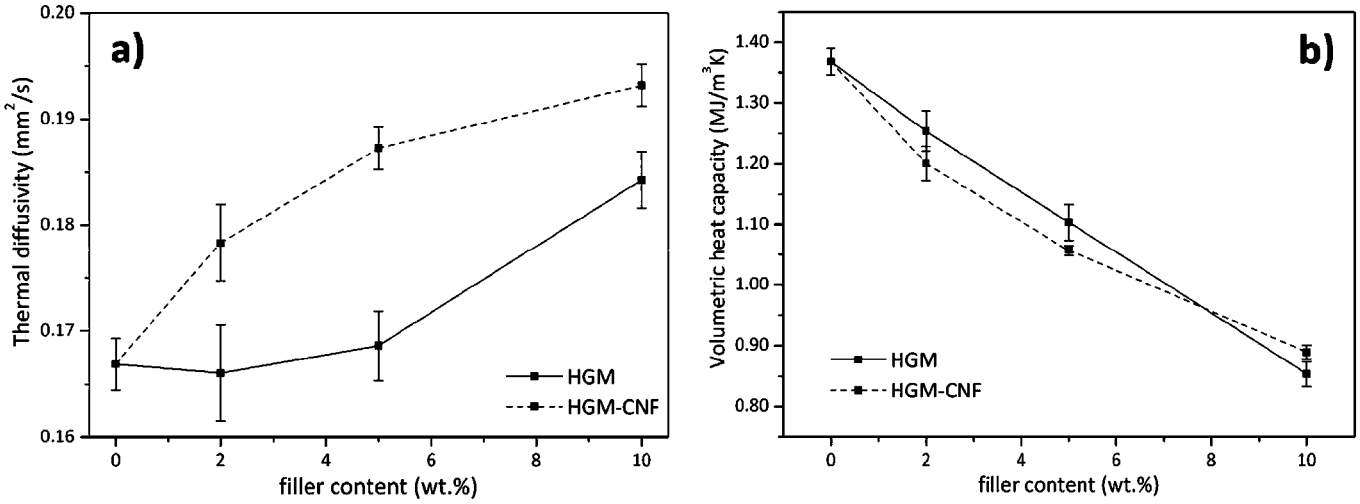

Fig. 6. a) Thermal diffusivity and b) volumetric heat capacity of the HGM and HGM-CNF composites, obtained by hot disk technique.

composites, the thermal diffusivity of the samples rapidly increases as the amount of hybrid microspheres increases (Fig. 6a). According to results reported for polymers filled with CNTs [52–55], the addition of CNTs resulted in an increased thermal diffusivity of the composite.

The ability to store thermal energy is expressed by the volumetric heat capacity, ρc. For the matrix, it was found that $\rho c = 1.37 \times 10^{-6}$ J/m^{3}K. The value of ρc for the HGMs is unknown. However, it is known that glass has a ρc of 1.98×10^{-6} J/m^{3}K while light gases presents extremely low values of volumetric heat capacity, i.e. 1.2×10^{-8} for air and 1.1×10^{-8} for Ar [51].

Thus, the HGM composites exhibit a lower ability to store thermal energy than the matrix (Fig. 6b). From the volumetric heat capacity values measured for the HGM-CNF composites, it was obtained that the behaviour was similar to that of the HGM composites, although the values were slightly lower than in the HGM composites, probably due to the CNFs. Further work should be done to understand the behaviour and properties of the hybrid material.

3.4. Electrical conductivity

The electrical conductivity of the resin, the HGM composites and the 2 and 5 wt.% HGM-CNF was lower than 1×10^{-7} S/m, which is the minimum value that can be measured with the equipment and the sample dimensions used. In the case of the HGM-CNF composites, an electrical conductivity of $7 \pm 3 \times 10^{-4}$ S/m and $3 \pm 2 \times 10^{-4}$ S/m was obtained for the 10 wt.% HGM-CNF composite in the through-thickness and in-plane directions, respectively (Supplementary Information). Taking into account the results obtained from the TGA of the hybrid materials obtained by CVD, this result implies that the critical amount of HGM-CNF at which takes place the formation of a continuous electrically conducting network within the resin [45] is between about 1.25 and 2.5 wt.% of CNFs, which corresponds to the composites with 5 and 10 wt.% of HGMs-CNFs, respectively. By assuming that the CNFs synthesized by CVD had mainly grown on the surface of the HGMs, an HGM-CNF can be modelled as a hybrid particle of single-phase material. The theoretical percolation threshold should be 4.9 wt.%. The followed procedure and the applied equations are available in the Supplementary Information. The experimental percolation threshold obtained in this work is higher than the theoretical value; this could be because the CNFs do not completely cover the surface of the HGMs, or due to the size distribution of HGM. The obtained result is a good first approximation to the experimental percolation threshold obtained in this study, which is located between 5 and 10 wt.% of HGMs-CNFs.

4. Conclusions

The thermal and electrical behaviour of as-received HGMs and synthesized HGMs-CNFs composites were studied to assess the effect of the HGMs on the resin and the effect of the CNFs on the HGM composites. These HGMs-CNFs mainly consist of HGMs surrounded by carbon nanofibers and were synthesized in our lab by using chemical vapour deposition.

Both types of composites were directly prepared by hand mixing. Although the hybrid microspheres have carbon-based nanomaterials, no further dispersing step or dispersing aiding agents were needed. The quality of both composites, in terms of matrix porosity and filler dispersion, was similar to that in the reported literature.

By adding 10% wt. HGM-CNFs to a high temperature resin (thermal stability up to *ca.* 350 °C) we can obtain a low density (0.823 g/cm^3), low thermally (0.172 W/mK) and good electrically conducting ($7 \pm 3 \times 10^{-4}$ S/m) composite. This material presents an unusual combination of properties, such as a low thermal conductivity and a relatively high electrical conductivity. This new generation of hybrid nanofillers paves the way to unique composite materials with properties that are currently hard to combine in a single material.

Acknowledgments

This work was supported by the European Commission under the 7th Framework Program, NFRP project (PICIG12-GA-2012-33924), ROBOHEALTH-A project (DPI2013-47944-C4-1-R) funded by Spanish Ministry of Economy and Competitiveness and from the RoboCity2030-II-CM project (S2009/DPI-1559), funded by "Programas de Actividades I+D en la Comunidad de Madrid" and co-funded by Structural Funds of the EU. R. G. V. gratefully acknowledges the Spanish Ministry of Science and Innovation for financial funding through the Ramon y Cajal Fellowship. L. C. H-R acknowledges the support from the Spanish Ministry of Education through the FPU programme (FPU14/06843). The authors would like to acknowledge 3M for providing the hollow glass microspheres, Scott Bader for providing the resin and J. C. Fernandez for the as-received HGM composite preparation.

Appendix A. Supplementary data

Supplementary data related to this article can be found at http://dx.doi.org/10.1016/j.compscitech.2017.08.020.

References

[1] I. Krupa, V. Cecen, A. Boudenne, J. Prokeš, I. Novák, The mechanical and adhesive properties of electrically and thermally conductive polymeric composites based on high density polyethylene filled with nickel powder, Mater. Des. 51 (2013) 620–628, http://dx.doi.org/10.1016/j.matdes.2013.03.067.
[2] Y.P. Mamunya, V.V. Davydenko, P. Pissis, E.V. Lebedev, Electrical and thermal conductivity of polymers filled with metal powders, Eur. Polym. J. 38 (2002) 1887–1897, http://dx.doi.org/10.1016/S0014-3057(02)00064-2.
[3] A. Yu, P. Ramesh, X. Sun, E. Bekyarova, M.E. Itkis, R.C. Haddon, Enhanced thermal conductivity in a hybrid graphite nanoplatelet - carbon nanotube filler for epoxy composites, Adv. Mater 20 (2008) 4740–4744, http://dx.doi.org/10.1002/adma.200800401.
[4] S.Y. Kwon, I.M. Kwon, Y.-G. Kim, S. Lee, Y.-S. Seo, A large increase in the thermal conductivity of carbon nanotube/polymer composites produced by percolation phenomena, Carbon 55 (2013) 285–290, http://dx.doi.org/10.1016/j.carbon.2012.12.063.
[5] H. Chen, V.V. Ginzburg, J. Yang, Y. Yang, W. Liu, Y. Huang, L. Du, B. Chen, Thermal conductivity of polymer-based composites: fundamentals and applications, Prog. Polym. Sci. 59 (2016) 41–85, http://dx.doi.org/10.1016/j.progpolymsci.2016.03.001.
[6] Y. Hu, G. Du, N. Chen, A novel approach for Al2O3/epoxy composites with high strength and thermal conductivity, Compos. Sci. Technol. 124 (2016) 36–43, http://dx.doi.org/10.1016/j.compscitech.2016.01.010.
[7] M. Donnay, S. Tzavalas, E. Logakis, Boron nitride filled epoxy with improved thermal conductivity and dielectric breakdown strength, Compos. Sci. Technol. 110 (2015) 152–158, http://dx.doi.org/10.1016/j.compscitech.2015.02.006.
[8] K.C. Yung, B.L. Zhu, T.M. Yue, C.S. Xie, Preparation and properties of hollow glass microsphere-filled epoxy-matrix composites, Compos. Sci. Technol. 69 (2009) 260–264, http://dx.doi.org/10.1016/j.compscitech.2008.10.014.
[9] R. Sun, H. Yao, H.-B. Zhang, Y. Li, Y.-W. Mai, Z.-Z. Yu, Decoration of defect-free graphene nanoplatelets with alumina for thermally conductive and electrically insulating epoxy composites, Compos. Sci. Technol. 137 (2016) 16–23, http://dx.doi.org/10.1016/j.compscitech.2016.10.017.
[10] J.-W. Zha, T.-X. Zhu, Y.-H. Wu, S.-J. Wang, R.K.Y. Li, Z.-M. Dang, Tuning of thermal and dielectric properties for epoxy composites filled with electrospun alumina fibers and graphene nanoplatelets through hybridization, J. Mater Chem. C 3 (2015) 7195–7202, http://dx.doi.org/10.1039/C5TC01552A.
[11] W. Cui, F. Du, J. Zhao, W. Zhang, Y. Yang, X. Xie, Y.-W. Mai, Improving thermal conductivity while retaining high electrical resistivity of epoxy composites by incorporating silica-coated multi-walled carbon nanotubes, Carbon 49 (2011) 495–500, http://dx.doi.org/10.1016/j.carbon.2010.09.047.
[12] N. Gupta, D. Pinisetty, A review of thermal conductivity of polymer matrix syntactic foams—effect of hollow particle wall thickness and volume fraction, JOM 65 (2013) 234–245, http://dx.doi.org/10.1007/s11837-012-0512-0.
[13] B.L. Zhu, H. Zheng, J. Wang, J. Ma, J. Wu, R. Wu, Tailoring of thermal and dielectric properties of LDPE-matrix composites by the volume fraction,

density, and surface modification of hollow glass microsphere filler, Compos. Part B Eng. 58 (2014) 91–102, http://dx.doi.org/10.1016/j.compositesb.2013.10.029.
[14] B. Zhu, J. Ma, J. Wang, J. Wu, D. Peng, Thermal, dielectric and compressive properties of hollow glass microsphere filled epoxy-matrix composites, J. Reinf. Plast. Compos 31 (2012) 1311–1326, http://dx.doi.org/10.1177/0731684412452918.
[15] J.Z. Liang, F.H. Li, Heat transfer in polymer composites filled with inorganic hollow micro-spheres: a theoretical model, Polym. Test. 26 (2007) 1025–1030, http://dx.doi.org/10.1016/j.polymertesting.2007.07.002.
[16] N. Gupta, R. Ye, M. Porfiri, Comparison of tensile and compressive characteristics of vinyl ester/glass microballoon syntactic foams, Compos. Part B Eng. 41 (2010) 236–245, http://dx.doi.org/10.1016/j.compositesb.2009.07.004.
[17] N. Gupta, R. Nagorny, Tensile properties of glass microballoon-epoxy resin syntactic foams, J. Appl. Polym. Sci. 102 (2006) 1254–1261, http://dx.doi.org/10.1002/app.23548.
[18] M. Colloca, N. Gupta, M. Porfiri, Tensile properties of carbon nanofiber reinforced multiscale syntactic foams, Compos. Part B Eng. 44 (2013) 584–591, http://dx.doi.org/10.1016/j.compositesb.2012.02.030.
[19] R.L. Poveda, N. Gupta, Electrical properties of carbon nanofiber reinforced multiscale polymer composites, Mater. Des. 56 (2014) 416–422, http://dx.doi.org/10.1016/j.matdes.2013.11.074.
[20] R.L. Poveda, S. Achar, N. Gupta, Viscoelastic properties of carbon nanofiber reinforced multiscale syntactic foam, Compos. Part B Eng. 58 (2014) 208–216, http://dx.doi.org/10.1016/j.compositesb.2013.10.079.
[21] R.L. Poveda, G. Dorogokupets, N. Gupta, Carbon nanofiber reinforced syntactic foams: degradation mechanism for long term moisture exposure and residual compressive properties, Polym. Degrad. Stab. 98 (2013) 2041–2053, http://dx.doi.org/10.1016/j.polymdegradstab.2013.07.007.
[22] R.L. Poveda, S. Achar, N. Gupta, Thermal expansion of carbon nanofiber-reinforced multiscale polymer composites, JOM 64 (2012) 1148–1157, http://dx.doi.org/10.1007/s11837-012-0402-5.
[23] H. Qian, A. Bismarck, E.S. Greenhalgh, M.S.P. Shaffer, Synthesis and characterisation of carbon nanotubes grown on silica fibres by injection CVD, Carbon 48 (2010) 277–286, http://dx.doi.org/10.1016/j.carbon.2009.09.029.
[24] S.S. Wicks, R.G. de Villoria, B.L. Wardle, Interlaminar and intralaminar reinforcement of composite laminates with aligned carbon nanotubes, Compos. Sci. Technol. 70 (2010) 20–28, http://dx.doi.org/10.1016/j.compscitech.2009.09.001.
[25] N. Yamamoto, A. John Hart, E.J. Garcia, S.S. Wicks, H.M. Duong, A.H. Slocum, B.L. Wardle, High-yield growth and morphology control of aligned carbon nanotubes on ceramic fibers for multifunctional enhancement of structural composites, Carbon 47 (2009) 551–560, http://dx.doi.org/10.1016/j.carbon.2008.10.030.
[26] Z.H. Han, B. Yang, S.H. Kim, M.R. Zachariah, Application of hybrid sphere/carbon nanotube particles in nanofluids, Nanotechnology 18 (2007) 105701.
[27] Q. Zhang, J. Huang, F. Wei, G. Xu, Y. Wang, W. Qian, D. Wang, Large scale production of carbon nanotube arrays on the sphere surface from liquefied petroleum gas at low cost, Chin. Sci. Bull. 52 (2007) 2896–2902, http://dx.doi.org/10.1007/s11434-007-0458-8.
[28] D. He, M. Bozlar, M. Genestoux, J. Bai, Diameter- and length-dependent self-organizations of multi-walled carbon nanotubes on spherical alumina microparticles, Carbon 48 (2010) 1159–1170, http://dx.doi.org/10.1016/j.carbon.2009.11.039.
[29] D. He, H. Li, J. Bai, Experimental and numerical investigation of the position-dependent growth of carbon nanotube–alumina microparticle hybrid structures in a horizontal CVD reactor, Carbon 49 (2011) 5359–5372, http://dx.doi.org/10.1016/j.carbon.2011.08.003.
[30] R.N. Othman, I.A. Kinloch, A.N. Wilkinson, Synthesis and characterisation of silica–carbon nanotube hybrid microparticles and their effect on the electrical properties of poly(vinyl alcohol) composites, Carbon 60 (2013) 461–470, http://dx.doi.org/10.1016/j.carbon.2013.04.062.
[31] S. Huang, Growing carbon nanotubes on patterned submicron-size SiO2 spheres, Carbon 41 (2003) 2347–2352, http://dx.doi.org/10.1016/S0008-6223(03)00275-6.
[32] E.F. Zegeye, E. Woldesenbet, Processing and mechanical characterization of carbon nanotube reinforced syntactic foams, J. Reinf. Plast. Compos 31 (2012) 1045–1052, http://dx.doi.org/10.1177/0731684412452919.
[33] P. Romero, R. Oro, M. Campos, J.M. Torralba, R. Guzman de Villoria, Simultaneous synthesis of vertically aligned carbon nanotubes and amorphous carbon thin films on stainless steel, Carbon 82 (2015) 31–38, http://dx.doi.org/10.1016/j.carbon.2014.10.020.
[34] ASTM D792-13, Standard Test Methods for Density and Specific Gravity (Relative Density) of Plastics by Displacement, ASTM International, West Conshohocken, PA, 2013, http://dx.doi.org/10.1520/D0792.
[35] S.E. Gustafsson, Transient plane source techniques for thermal conductivity and thermal diffusivity measurements of solid materials, Rev. Sci. Instrum. 62 (1991) 797.
[36] Y. He, Rapid thermal conductivity measurement with a hot disk sensor: Part 1. Theoretical considerations, Thermochim. Acta 436 (2005) 122–129, http://dx.doi.org/10.1016/j.tca.2005.06.026.
[37] S.A. Al-Ajlan, Measurements of thermal properties of insulation materials by using transient plane source technique, Appl. Therm. Eng. 26 (2006) 2184–2191, http://dx.doi.org/10.1016/j.applthermaleng.2006.04.006.
[38] J.E. Shelby, Introduction to Glass Science and Technology, Royal Society of Chemistry, 2005.
[39] J.H. Lehman, M. Terrones, E. Mansfield, K.E. Hurst, V. Meunier, Evaluating the characteristics of multiwall carbon nanotubes, Carbon 49 (2011) 2581–2602, http://dx.doi.org/10.1016/j.carbon.2011.03.028.
[40] B. Scheibe, E. Borowiak-Palen, R.J. Kalenczuk, Oxidation and reduction of multiwalled carbon nanotubes — preparation and characterization, Mater. Charact. 61 (2010) 185–191, http://dx.doi.org/10.1016/j.matchar.2009.11.008.
[41] J. Li, X. Luo, X. Lin, Preparation and characterization of hollow glass microsphere reinforced poly(butylene succinate) composites, Mater. Des. 46 (2013) 902–909, http://dx.doi.org/10.1016/j.matdes.2012.11.054.
[42] T.C. Lin, N. Gupta, A. Talalayev, Thermoanalytical characterization of epoxy matrix-glass microballoon syntactic foams, J. Mater. Sci. 44 (2009) 1520–1527, http://dx.doi.org/10.1007/s10853-008-3074-3.
[43] J.C. Maxwell, A Treatise on Electricity and Magnetism, Clarendon Press, Oxford, 1873.
[44] H. Zhou, S. Zhang, M. Yang, The effect of heat-transfer passages on the effective thermal conductivity of high filler loading composite materials, Compos. Sci. Technol. 67 (2007) 1035–1040, http://dx.doi.org/10.1016/j.compscitech.2006.06.004.
[45] M.H. Al-Saleh, U. Sundararaj, A review of vapor grown carbon nanofiber/polymer conductive composites, Carbon 47 (2009) 2–22, http://dx.doi.org/10.1016/j.carbon.2008.09.039.
[46] A.A. Balandin, Thermal properties of graphene and nanostructured carbon materials, Nat. Mater 10 (2011) 569–581, http://dx.doi.org/10.1038/nmat3064.
[47] F. Gong, H.M. Duong, D.V. Papavassiliou, Inter-carbon nanotube contact and thermal resistances in heat transport of three-phase composites, J. Phys. Chem. C 119 (2015) 7614–7620, http://dx.doi.org/10.1021/acs.jpcc.5b00651.
[48] F. Gong, K. Bui, D.V. Papavassiliou, H.M. Duong, Thermal transport phenomena and limitations in heterogeneous polymer composites containing carbon nanotubes and inorganic nanoparticles, Carbon 78 (2014) 305–316, http://dx.doi.org/10.1016/j.carbon.2014.07.007.
[49] R.S. Prasher, X.J. Hu, Y. Chalopin, N. Mingo, K. Lofgreen, S. Volz, F. Cleri, P. Keblinski, Turning carbon nanotubes from exceptional heat conductors into insulators, Phys. Rev. Lett. 102 (2009), http://dx.doi.org/10.1103/PhysRevLett.102.105901.
[50] C.-W. Nan, R. Birringer, D.R. Clarke, H. Gleiter, Effective thermal conductivity of particulate composites with interfacial thermal resistance, J. Appl. Phys. 81 (1997) 6692.
[51] A. Salazar, On thermal diffusivity, Eur. J. Phys. 24 (2003) 351, http://dx.doi.org/10.1088/0143-0807/24/4/353.
[52] V. Datsyuk, M. Lisunova, M. Kasimir, S. Trotsenko, K. Gharagozloo-Hubmann, I. Firkowska, S. Reich, Thermal transport of oil and polymer composites filled with carbon nanotubes, Appl. Phys. A 105 (2011) 781–788, http://dx.doi.org/10.1007/s00339-011-6667-7.
[53] M. Akoshima, H. Abe, T. Baba, Thermal diffusivity of carbon materials as candidate reference materials, Int. J. Thermophys. 36 (2014) 2507–2517, http://dx.doi.org/10.1007/s10765-014-1624-2.
[54] J. Chiguma, E. Johnson, P. Shah, N. Gornopolskaya, W.E. Jones Jr., Thermal diffusivity and thermal conductivity of epoxy-based nanocomposites by the laser flash and differential scanning calorimetry techniques, Open J. Compos. Mater 03 (2013) 51–62, http://dx.doi.org/10.4236/ojcm.2013.33007.
[55] Y. Xu, G. Ray, B. Abdel-Magid, Thermal behavior of single-walled carbon nanotube polymer–matrix composites, Compos. Part Appl. Sci. Manuf. 37 (2006) 114–121, http://dx.doi.org/10.1016/j.compositesa.2005.04.009.